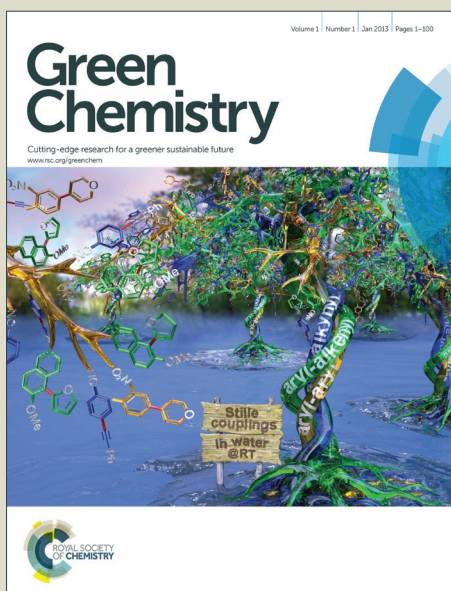


Green Chemistry

Accepted Manuscript



This is an *Accepted Manuscript*, which has been through the Royal Society of Chemistry peer review process and has been accepted for publication.

Accepted Manuscripts are published online shortly after acceptance, before technical editing, formatting and proof reading. Using this free service, authors can make their results available to the community, in citable form, before we publish the edited article. We will replace this *Accepted Manuscript* with the edited and formatted *Advance Article* as soon as it is available.

You can find more information about *Accepted Manuscripts* in the [Information for Authors](#).

Please note that technical editing may introduce minor changes to the text and/or graphics, which may alter content. The journal's standard [Terms & Conditions](#) and the [Ethical guidelines](#) still apply. In no event shall the Royal Society of Chemistry be held responsible for any errors or omissions in this *Accepted Manuscript* or any consequences arising from the use of any information it contains.



Journal Name

ARTICLE

Low Temperature Hydrogenation of Pyrolytic Lignin over Ru/TiO₂: 2D HSQC and ¹³C NMR Study of Reactants and Products

Wen Chen,^{ab†} Daniel J. McClelland,^{b†} Ali Azarpira,^c John Ralph,^c Zhongyang Luo,^a George W. Huber^{*b}

Received 00th January 20xx,
Accepted 00th January 20xx

DOI: 10.1039/x0xx00000x

www.rsc.org/

Pyrolytic lignin and hydrogenated pyrolytic lignin were characterized by 2D ¹H–¹³C HSQC and quantitative ¹³C NMR techniques. The pyrolytic lignin was produced from a mixed maple wood feedstock and separated from the bio-oil by water extraction. *p*-hydroxyphenyl (H), guaiacyl (G), and syringyl (S) aromatics were the basic units of pyrolytic lignin. The native lignin β-aryl ether, phenylcoumaran and resinol structures were not present in the pyrolytic lignin. The hydrogenation was conducted with a Ru/TiO₂ catalyst at temperatures ranging from 25–150 °C with higher temperatures exhibiting higher levels of hydrogenation. Solid coke formed on the catalyst surface (1% coke yield) even for hydrogenation at 25 °C. The carbon yield of pyrolytic lignin to coke increased from 1% to 5% as the hydrogenation temperature increased from 25 to 150 °C. A single-step hydrogenation at 150 °C resulted in a reduction from 65% to 39% aromatic carbons. A three-step hydrogenation scheme at this same temperature resulted in a reduction of aromatic carbons from 65% to 17%. The decrease in the aromatic carbon corresponded with an increase in the aliphatic carbon. Coke formation reduced from a 4.9% carbon yield of pyrolytic lignin in the first hydrogenation step to a 1% carbon yield in each of the second and third hydrogenation steps. The pyrolytic lignin could be separated into a high and low molecular weight fraction. The coke yield from the high molecular weight fraction was twice as much as that from the low molecular weight fraction.

Introduction

Fast pyrolysis of biomass combined with hydrodeoxygenation (HDO) of the fast pyrolysis produced bio-oil has been proposed as a low cost technology for the production of lignocellulosic fuels.^{1–5} Techno-economic analyses have shown that pyrolysis-HDO based approaches to biomass conversion have lower capital and operating costs than gasification and fermentation technologies.^{6–8} However, little is known about the chemistry that occurs during HDO due to the complicated reactions that are occurring in this process.^{9–12} The HDO approach has several challenges including low liquid product yields, reactor plugging, and high coke yields.^{10,13,14} This arises from the complexity of the bio-oil or pyrolysis oil which is a complicated emulsion that contains over 400 different compounds.¹⁵ Pyrolysis oil can be phase-separated into water-soluble and water-insoluble fractions by extraction with water.¹⁶ Upgrading the fractions separately may allow for better understanding of the HDO chemistry of each fraction and the bio-oil as a whole. The water-soluble fraction

of bio-oil contains sugars, anhydrosugars, acetic acid, hydroxyacetone, hydroxyacetaldehyde, furfural, and small amounts of phenolics.^{16,17} We have previously reported on the catalytic chemistry involved in the hydrogenation and HDO of the water-soluble fraction.^{17–20}

Less is known about the water-insoluble phase or the pyrolytic lignin. The phase mainly consists of phenolic oligomers derived from thermal depolymerization of the lignin fraction of the biomass source.²¹ Pyrolytic lignin is difficult to hydrotreat due to rapid polymerization of the complex high molecular weight aromatic structures that comprise it.²² The analysis of the pyrolytic lignin is extremely difficult. Pyrolytic lignin is not volatile which makes GC analysis not possible without functionalizing the pyrolytic lignin.²³ Spectroscopic techniques such as FTIR can give qualitative insights into functional groups in pyrolytic lignin.^{24–26} LC-MS is in principle possible, but remains less effective for the complex array of high molecular weight components. Gel permeation chromatography (GPC) can be used to give the approximate molecular weight of pyrolytic lignin.^{27–29} In contrast to the techniques mentioned above, NMR has the potential of providing quantitative (or at least comparative) and qualitative insights into pyrolytic lignin. ¹H and ¹³C NMR have been used to identify the primary functionality of the pyrolytic lignin.^{21,26,27,30,31} 2D ¹H–¹³C correlation (HSQC – heteronuclear single-quantum coherence) NMR has been used to provide more detailed information about the substructures in lignin, however this technique has not been used for the analysis of pyrolytic lignin.^{32–34} As we will show in this publication HSQC NMR can be used to show the absence of β-aryl ether, phenylcoumaran,

^a State Key Laboratory of Clean Energy Utilization, Zhejiang University, Hangzhou, 310027, PR China.

^b Department of Chemical and Biological Engineering, University of Wisconsin-Madison, Madison, WI 53706, USA. Email: gwhuber@wisc.edu

^c Department of Biochemistry, DOE Great Lakes Bioenergy Research Center, and Department of Biological Systems Engineering, University of Wisconsin, Madison, Wisconsin, 53726, USA

[†] Authors contributed equally to the production of this paper

* Corresponding Author

Electronic Supplementary Information (ESI) available: Additional figures and tables included in supplementary information. See DOI: 10.1039/x0xx00000x

and resinol structures in pyrolytic lignin as well as the disappearances of G and S units during hydrogenation of pyrolytic lignin. Meier et al.^{27,35-37} analyzed the structures of pyrolytic lignin using GPC, PY-GC/MS, FTIR, ¹³C NMR, and MS. They proposed five chemical structures ranging from a tetramer to an octamer with typical oligomers containing biphenyl, phenylcoumaran, diphenyl ether, stilbene, and resinol functionalities in them.

There are a limited number of papers that have reported on the HDO of pyrolytic lignin using Pd/C, Ru/C, or Pt/C in batch reactors.^{22,26,38,39} Hydrodeoxygenation of lignin and lignin model compounds have been studied; however, pyrolytic lignin has differences in both subunit linkages and functionalities from both the native lignins and the model compounds.^{40,41} The previous studies focused on the analysis of the final products from hydrotreating of pyrolytic lignin and did not identify the pyrolytic lignin-derived intermediates. Recent studies have focused on stabilization of bio-oil fractions in an effort to reduce the formation of solids during aging as well as prevent coke formation in further hydrotreating reactions.^{26,42} Rover et al. recently reported that phenolic bio-oil fractions similar to pyrolytic lignin could be hydrogenated at room temperature and 1 bar over a Pd/C catalyst to saturate bio-oil compounds and produce a more stable product. They observed a 25.5% to 350% increase in aliphatic proton resonances through semi-quantitative ¹H NMR.²⁶ Elliot et al. also recently reported that a two stage hydrotreating scheme of phenolic bio-oil fractions, a lower temperature Ru/C stabilization followed by a higher temperature Pd/C hydrogenation, removed heteroatoms with up to a 81% carbon yield.⁴²

The objective of this paper is to begin to develop a fundamental understanding of the chemistry that occurs during low temperature hydrogenation of pyrolytic lignin using HSQC and quantitative ¹³C NMR. Understanding this chemistry will allow us to design more efficient catalytic processes for the production of fuels and chemicals from bio-oils.

Experimental

Preparation and fractionation of pyrolytic lignin

Pyrolytic lignin was obtained by water extraction of pyrolysis bio-oil obtained from mixed hard woods. The mixed hardwood was obtained from the Cersosimo Lumber Company located in Brattleboro, VT harvested from various parts of the New England region. The bio-oil was collected from the 6th and 7th condenser of a fast pyrolysis Auger reactor.^{43,44} The bio-oil was stored in the refrigerator to minimize ageing. The bio-oil appeared as one single phase prior to separating it into various components. The procedure used for separation of the pyrolytic lignin from the bio-oil, modified from work by Oasmaa and Kuoppala,^{28,29} is shown in Figure 1. In brief, 5 g of bio-oil was added dropwise to 40 g of deionized water in a 50 mL centrifuge tube. The mixture was shaken then centrifuged at 7500 rpm (6603 rcf) in an Eppendorf Centrifuge 5430R v 2.2 for 40 min. After centrifuging, two phases, a light yellow-orange, water-soluble phase and a black, viscous, water-insoluble phase (pyrolytic lignin), were formed and separated by decanting.

The pyrolytic lignin was further fractionated by organic solvent extraction. Dichloromethane was added to the pyrolytic lignin which was shaken and centrifuged with the same method that was used for centrifuging the bio-oil. Two fractions formed, a dichloromethane-soluble fraction and a dichloromethane-insoluble fraction. The dichloromethane-soluble fraction was decanted off and collected. This was repeated two more times for the insoluble fraction using a total of 18 g of dichloromethane for 2.4 g of pyrolytic lignin for the fractionation. Oasmaa et al.^{29,45} showed that the dichloromethane-insoluble fraction had a 1.5 times higher molecular weight than the dichloromethane-soluble fraction by using GPC. In this paper, the dichloromethane-soluble fraction and the dichloromethane-insoluble fraction were designated as the low molecular weight fraction (LMW fraction) and the high molecular weight fraction (HMW fraction), respectively. After fractionation, the dichloromethane was removed by a 24 h evaporation step at 50 °C for the LMW fraction and at 20 °C for the HMW fraction. The pyrolytic lignin and pyrolytic lignin fraction solutions were kept under refrigeration and hydrogenated or analyzed within two weeks of preparation.

Hydrogenation of pyrolytic lignin and biphenyl activity testing

Pyrolytic lignin is a black viscous material with a smoky odor. It is soluble in ethanol (up to 15 wt%), and hence ethanol was used as the reaction solvent. Reactions were carried out in a 50 mL HEL batch reactor which had a pressure gauge, two inlet/outlet valves, and a pressure relief valve. The HEL batch reactor was placed in an electric heating well/magnetic stirrer with a controller to control the temperature, temperature ramp rate, and stir speed of a magnetic stir bar. The catalyst used in the experiments was Ru/TiO₂ prepared by incipient wetness impregnation. This catalyst was chosen due to the high activity of ruthenium for hydrogenation reactions compared to other metals (Pd, Rh, Pt, Ni, Co)^{20,46} and the high hydrothermal stability of titania.⁴⁷ Titanium(IV) oxide (Sigma-Aldrich catalog number 718467) and ruthenium(III) nitrosyl nitrate solution (Sigma-Aldrich catalog number 373567) were used as the support and

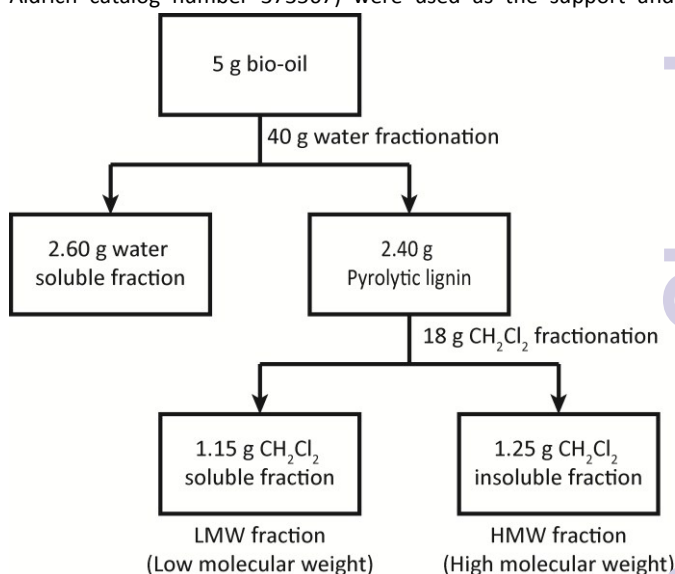


Figure 1. Fractionation of bio-oil into water-soluble, LMW, and HMW pyrolytic lignin fractions

precursor for the preparation of Ru/TiO₂. ICP-AES was conducted by Galbraith Laboratories, Inc. The catalyst was determined to be 2.80 wt% Ru. The CO uptake of the catalyst was 16.63 μmol/g as measured using CO pulse chemisorption on a Micromeritics Autochem II 2920. Prior to the experiment, 1.50 g of catalyst was reduced in the reactor. The feed, 10 g of 10 wt% pyrolytic lignin in ethanol, was added to the reactor which was then purged with 725 psig of H₂ five times and pressurized with H₂ to 725 psig. The reactor was then heated at a ramp rate of 10 °C/min to 150 °C/min and held for a reaction time of 2.5 h. The solution was stirred at 700 rpm for the duration of the heating phase and reaction. After completion of the reaction, the reactor was quenched to room temperature for collection and analysis of the products.

Biphenyl was used to test the hydrogenation activity of the fresh and spent catalysts. The activity test comprised of reacting 10 g of 10 wt% biphenyl in *n*-hexane over a fresh or spent catalyst at 150 °C and 725 psig H₂. The procedure was the same as the pyrolytic hydrogenation except the reaction was held for 1.0 h instead of 2.5 h.

Product analysis

The pressure after reaction was recorded to measure the amount of hydrogen consumed. The gaseous products were collected using a gas bag and analyzed using a Shimadzu GC2014 equipped with two parallel lines: 1) a Restek RTX–Alumina column connected to a flame ionization detector (FID) to analyze hydrocarbons (CH₄, C₂–C₅ alkanes and olefins) and 2) a RTX–MS-5A column followed by a RTX-Q-plot with a thermal conductivity detector (TCD) to analyze CO and CO₂.

After hydrogenation a single phase reddish-brown transparent liquid was obtained. The liquid product and recovered catalyst were collected and separated by filtration. The liquid product was separated by rotary evaporation at 55 °C and 2.5 psi (170 mbar) for 1 h. The distillate and residue are designated as volatile liquids and non-volatile liquids respectively.

The non-volatile liquids were characterized by quantitative 1D ¹³C and 2D HSQC NMR. The NMR samples were prepared by dissolving the non-volatile liquids in DMSO-*d*₆ with benzaldehyde as an internal standard. The wt% of non-volatile liquids, DMSO-*d*₆, and benzaldehyde were 25%, 72.5%, and 2.5%. All NMR experiments were carried out on a Bruker Biospin (Billerica, MA) AVANCE 500 MHz spectrometer fitted with a cryogenically cooled 5 mm DCH (¹³C-optimized) gradient probe. Quantitative ¹³C NMR spectra were obtained by using an inverse-gated decoupling pulse sequence, a 90° pulse, a relaxation delay of 12 s, a sweep width of 350 ppm, a TD of 87714, and 1024 scans. In the quantitative ¹³C NMR spectra, the relative peak area of the carbonyl group from benzaldehyde was set to 1. The HSQC experiment used the Bruker standard pulse sequence 'hsqcetgp' with the following parameters: 16 ppm sweep width (±6 ppm due to automated sweep width adjustment of the spectrometer) in F2 (¹H) with a TD2 of 2166, 220 ppm sweep width in F1 (¹³C) with a TD1 of 352, 24 scans, a 1.5 s relaxation delay, and with the evolution time set for a 1-bond ¹H–¹³C coupling constant of 145 Hz, with a total acquisition time of 3 h. Processing utilized 4096×1024 FFT, cosinebell-squared apodization in F1, Gaussian

multiplication apodization in F2, and linear prediction in neither dimension.

A total organic carbon analyzer (TOC; Shimadzu TOC-V_{CPH}) with a solid sample module (Shimadzu SSM-5000A) was utilized to determine the total carbon content of the pyrolytic lignin, its fractions, the non-volatile liquid product, and spent catalyst. Together with the quantitative ¹³C NMR, TOC was used to determine carbon yields of the hydrogenation products.

The liquid products were qualitatively analyzed on a GCMS-QP2010S (Shimadzu) equipped with a Restek-VMS column. The operating conditions were as follows: 1) hold for 5 min at 35 °C, 2) heat to 140 °C at 5 °C/min, 3) heat to 230 °C at 50 °C/min, and 4) hold for 20 min at 230 °C. Less than 2% of the carbon in the liquid products and non-volatile liquids of pyrolytic lignin, its fractions, and hydrogenated pyrolytic lignin was detected with GCMS.

The liquid products from the biphenyl hydrogenation were analyzed by Shimadzu GC2010 system with an Agilent HP INNOWAY column (60 m, 0.32 mm, 0.5 μm) and a FID. The following GC conditions were used: 1) hold for 10 min at 70 °C, 2) heat to 95 °C at 2 °C/min, 3) heat to 240 °C at 15 °C/min and 4) hold for 10 min at 240 °C.

The recovered catalyst was washed with acetone until the filtrate was colorless. Prior to coke analysis, the washed catalyst was rinsed three times with water and dried in the oven overnight at 110 °C. The dried catalyst was then run through the TOC to determine the mass of carbon as coke per mass of the spent catalyst. This allowed for the total moles of carbon as coke to be determined and with Equation 4, the carbon yield to coke.

The mass and moles of carbon in volatile liquids from pyrolytic lignin were estimated according to Equations 1 and 2.

$$\text{Mass of volatile liquids} = M_{\text{EL}} - M_{\text{LP}} * W_{\text{eth}} \quad (1)$$

$$\text{Moles of carbon in volatile liquids} = \frac{(M_{\text{EL}} - M_{\text{LP}} * W_{\text{eth}}) * C_{\text{eth}}}{\text{MW}_{\text{C}}} \quad (2)$$

where M_{EL} is the mass of liquids evaporated during rotary evaporation, M_{LP} is the mass of the liquid product, W_{eth} is the weight percentage of ethanol in the feedstock, C_{eth} is the weight percentage of carbon in ethanol, and MW_{C} is the molecular weight of elemental carbon. The weight percentage of carbon in the volatile liquids was assumed to be similar to that of ethanol.

The mass and carbon yields of volatile liquids, non-volatile liquids, and coke from pyrolytic lignin were calculated according to Equations 3 and 4.

$$\text{Mass yield} = \frac{M_{\text{P}}}{M_{\text{PL}}} \times 100\% \quad (3)$$

$$\text{Carbon yield} = \frac{n_{\text{C,P}}}{n_{\text{C,PL}}} \times 100\% \quad (4)$$

where M_{SP} is the mass of a product, M_{PL} is the mass of the pyrolytic lignin in the feed, $n_{\text{C,P}}$ is the moles of carbon in the same product, and $n_{\text{C,PL}}$ is the moles of carbon in the pyrolytic lignin feed.

Results and discussion

Characterization of pyrolytic lignin and its fractions by NMR

Two dimensional HSQC NMR experiments have the ability to resolve otherwise overlapping resonances observed in either of the 1D ¹H or

ARTICLE

Journal Name

^{13}C NMR spectra.^{33,34} The HSQC spectra of the pyrolytic lignin is shown in Figure 2. This figure can be divided up into three regions, 1) the aromatic region ($\delta_{\text{C}}/\delta_{\text{H}}$ 95-145/6-8.25), 2) the aliphatic C–O region ($\delta_{\text{C}}/\delta_{\text{H}}$ 50-95/2.75-6.0), and 3) the aliphatic C–C region ($\delta_{\text{C}}/\delta_{\text{H}}$ 5-50/0.5-3.0). These three regions are displayed in more detail in Figures 3, 4, and 5.

HSQC correlation signals from the pyrolytic lignin were compared with published data for lignin structures.⁴⁸⁻⁵³ The pyrolytic lignin, LMW fraction, HMW fraction, and three-step hydrogenated pyrolytic lignin are characterized by 2D ^1H – ^{13}C HSQC NMR in combination with quantitative ^{13}C NMR as shown in the supporting information (Figure S1). Figure 3 shows the aromatic region for the pyrolytic lignin, the LMW fraction, the HMW fraction, and the three-step hydrogenated pyrolytic lignin. The intense correlation signals between $\delta_{\text{C}}/\delta_{\text{H}}$ 128.0-136.0/7.40-8.00 derive from the protonated aromatic carbons of benzaldehyde that was added as an internal standard. The cross-signals at $\delta_{\text{C}}/\delta_{\text{H}}$ 105.5/6.42 are attributed to $\text{C}_{2,6}/\text{H}_{2,6}$ correlations of syringyl (S) units. From previous literature,^{32-34,54,55} $\delta_{\text{C}}/\delta_{\text{H}}$ 103.8/6.69 and 106.2/7.27 are attributed to $\text{C}_{2,6}/\text{H}_{2,6}$ positions of syringyl units in native lignin. Strong correlation signals at $\delta_{\text{C}}/\delta_{\text{H}}$ 112.8/6.70, 115.4/6.61, and 119.3/6.61 correspond to C_2/H_2 , C_5/H_5 , and C_6/H_6 correlations of guaiacyl (G) units. If present small correlations at $\delta_{\text{C}}/\delta_{\text{H}}$ 129.3/6.91-7.15 would correlate to $\text{C}_{2,6}/\text{H}_{2,6}$ from *p*-hydroxyphenyl (H) units. The correlations of the $\text{H}_{3,5}$ position overlap with those from $\text{G}_{5/6}$ position. Slight changes in the chemical shifts in the aromatic region from previously reported signals^{32-34,54,55} to our observed signals might be due to interactions of other functional groups that are formed in the pyrolysis process, i.e., on the altered sidechain on the H, G, and S aromatic rings. The aromatic regions from pyrolytic lignin and LMW fraction are quite similar. The HMW spectra has a higher ratio of G to S units than the LMW and pyrolytic fractions. Signals in the HMW fraction are much broader than those in the LMW fraction, consistent with its higher molecular weight and slower molecular motion.²¹ Only S groups are observed in the aromatic region of the three-step hydrogenated pyrolytic lignin.

The aliphatic C–O regions in the HSQC spectra are presented in Figure 4. Signals from methoxyls ($\delta_{\text{C}}/\delta_{\text{H}}$ 55.7/3.75) and ethanol ($\delta_{\text{C}}/\delta_{\text{H}}$ 56.0/3.50) are the most prominent in this region. Lignin is a complex macromolecule synthesized from two main precursors, coniferyl, and sinapyl alcohols (with low levels from *p*-coumaryl alcohol),⁵⁶ in which the monomer-derived units are connected by several types of C–C or C–O–C linkages, including β –5, 5–5, β – β , β –O–4, and 4–O–5, forming phenylcoumaran, biphenyl, resinol, alkyl-aryl ether, and biphenyl ether substructures. β –O–4-linkages are involved in the predominant β -aryl ether units in lignin.⁵⁶ The β -aryl ether units have characteristic signals at $\delta_{\text{C}}/\delta_{\text{H}}$ 72.2/4.86 from $\text{C}_\alpha/\text{H}_\alpha$, 85.8/4.12, 86.8/3.99, or 83.9/4.29 from $\text{C}_\beta/\text{H}_\beta$, and $\delta_{\text{C}}/\delta_{\text{H}}$ 59.5-59.7/3.41-3.64 from $\text{C}_\gamma/\text{H}_\gamma$.^{32-34,54} These signals, along with those corresponding to the characteristic signals from resinols or phenylcoumarans, are not observed in the spectra shown in Figure 4. This is in accordance with previous pyrolysis studies that indicate that ether bonds in cyclic resinols and phenylcoumarans, and β –O–4-linkages in β -ethers are broken during pyrolysis.^{57,58} Our results differ from the work of Meier who did not use HSQC analysis but claimed that resinols and

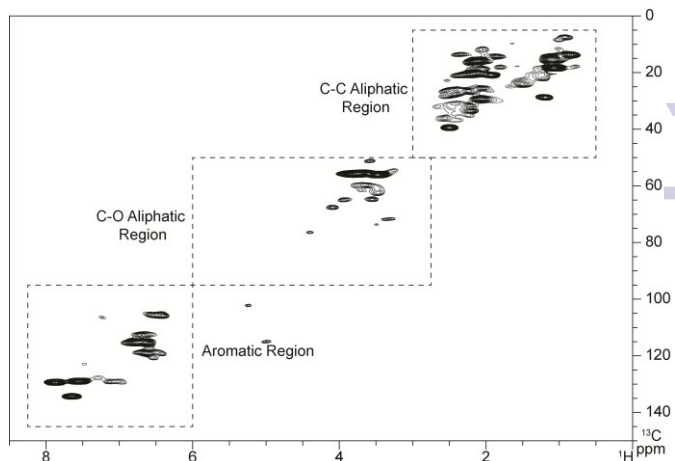


Figure 2. HSQC spectra of pyrolytic lignin highlighting the aliphatic C–C, aliphatic C–O, and aromatic regions.

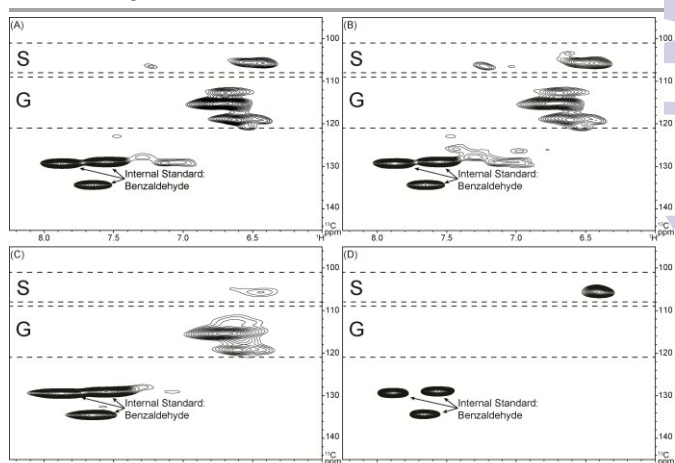


Figure 3. Aromatic regions of HSQC spectra from (A) pyrolytic lignin, (B) LMW pyrolytic lignin fraction, (C) HMW pyrolytic lignin fraction, and (D) three-step hydrogenated pyrolytic lignin

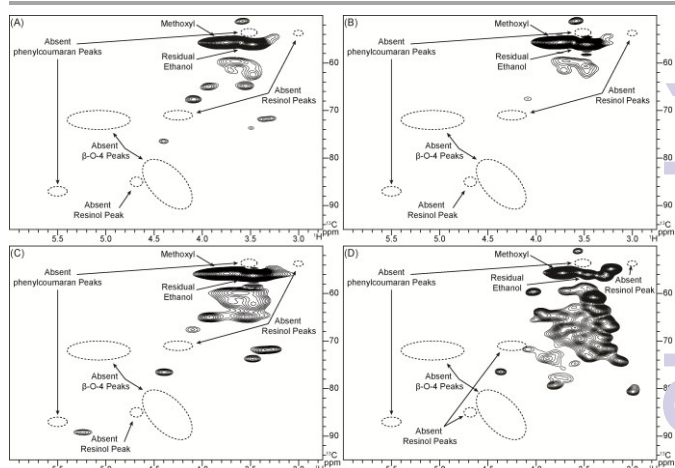


Figure 4. Aliphatic C–O regions of HSQC spectra from (A) pyrolytic lignin, (B) LMW pyrolytic lignin fraction, (C) HMW pyrolytic lignin fraction, and (D) three-step hydrogenated pyrolytic lignin. Positions of absent resinol, phenylcoumaran, and β –O–4 unit correlation peaks are shown by dotted circles.

phenylcoumarans were present in their pyrolytic lignin.^{36,37} In this region, the HMW fraction presents signals at $\delta_{\text{C}}/\delta_{\text{H}}$ 71.8/3.32, 73.8/3.48, 76.6/4.40, and 89.1/5.24, whereas the LMW fraction does not have these signals. This demonstrates that the C–O linkages

in LMW and HMW are different. The three-step hydrogenated pyrolytic lignin shows increases in both the number of signals and signal intensities. This is expected as G, H, and S aromatic units are converted to aliphatics during hydrogenation.

The aliphatic C–C regions of HSQC spectra are shown in Figure 5. The signal intensity in this region is higher than in the C–O region. Similar results have been reported with the ^{13}C NMR spectra of pyrolytic lignin from different feedstocks obtained by Scholze et al.²⁷ and Mullen et al.²¹ Pyrolytic lignin, the LMW fraction and the HMW fraction show similar spectra in this region. The three-step hydrogenated pyrolytic lignin spectra has many more signals in the aliphatic C–C region than the non-hydrogenated fractions.

Based on these results, it can be concluded that the aromatic units in pyrolytic lignin are primarily S and G with minor amounts of H. No evidence can be found for the formation of polynuclear aromatics such as naphthalenes indicating that such condensations are not prominent during lignin pyrolysis. Meier proposed several different dimeric substructures including biphenyl, phenylcoumaran, resinol, and diphenyl ether while Boateng et al.²¹ did not detect phenylcoumaran or resinol structures in their pyrolytic lignin. In this work, characteristic HSQC signals corresponding to phenylcoumaran and resinol structures are not evident. Both Meier and Boateng suggested the existence of biphenyl structures in which the two aromatics are linked by a 5–5'-bond. This structure was also identified in lignin and has the highest bonding dissociation energy among the various inter-unit linkages. This implies that this structure might be retained during pyrolysis although it could not be confirmed from 2D-HSQC or 1D ^{13}C NMR. Biphenyls are not easily detectable in 2D-HSQC due to the tertiary nature of the diagnostic 5-carbons (without a bonded hydrogen); in native lignins they are readily identified as they exist as dibenzodioxocins that has diagnostic α - and β -C/H correlations.^{59,60} Biphenyls could also not be identified in ^{13}C NMR spectra due to the large number of overlapping peaks in that region.

Two contrasting hypotheses have been proposed for the formation of high molecular weight pyrolytic lignin molecules, one by reactive boiling ejection⁶¹ and the other by depolymerisation to volatile monomers and repolymerization after escaping primary pyrolysis.⁵⁸ Teixeira et al. has shown reactive boiling ejection to be a mechanism for the production of anhydro-oligomers during pyrolysis

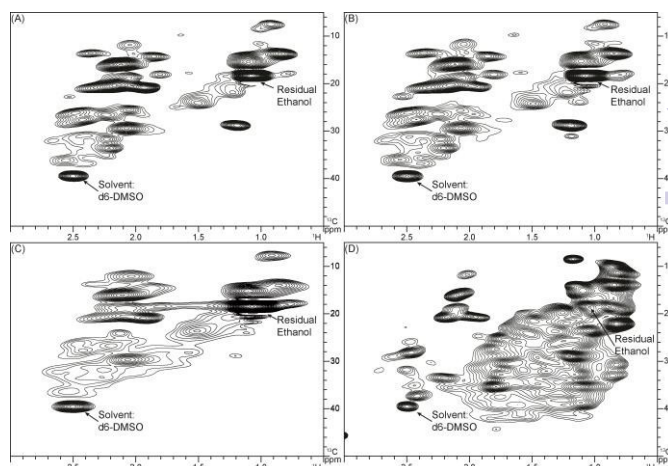


Figure 5. Aliphatic C–C regions of HSQC spectra from (A) pyrolytic lignin, (B) LMW pyrolytic lignin fraction, (C) HMW pyrolytic lignin fraction, and (D) three-step hydrogenated pyrolytic lignin.

of cellulose⁶¹ and involves an intermediate liquid cellulose which violently boils expelling liquid aerosols. The liquid aerosols become entrained in the gas phase allowing for transportation of the larger non-volatile molecules out of the pyrolysis bed. Further investigation of this method with lignin showed the formation of a lignin liquid phase but the ejection of particles could not be confirmed.⁶¹ Contrasting this, Patwardhan et al. has shown that pyrolysis of lignin yields up to 30.5% of monolignols with a 17% yield of CO and CO₂ and 37% yield of char. The accompanying bio-oil condensation conditions were shown to facilitate polymerization of the monolignols.⁵⁸ The absence of β -aryl ether, phenylcoumaran, and resinol structures in the pyrolytic lignin supports that depolymerisation occurs during pyrolysis.

Hydrogenation of pyrolytic lignin

Effect of temperature on hydrogenation of pyrolytic lignin

Pyrolytic lignin hydrogenation experiments at varying temperatures were conducted and analyzed as shown in Table 1. The gas product contained H₂ with a small amount of CH₄ and C₂H₆ at reaction temperatures over 100 °C. Ethanol reactivity was tested by the reaction of ethanol with Ru/TiO₂ at 150 °C resulting in a 13.8% carbon yield to CH₄ (53.6 mmol) and 3.6% carbon yield to C₂H₆ (7.0 mmol) from ethanol. The amounts of CH₄ and C₂H₆ produced with pure ethanol was over 30 times more than during hydrogenation of

Table 1. Gas products and carbon balance for hydrogenation of pyrolytic lignin at different reaction temperatures (Reaction condition: 725 psig of initial H₂ pressure, 2.5 h reaction time, 10 g of pyrolytic lignin in ethanol (10 wt%), 1.50 g Ru/TiO₂).

Reaction temperature (°C)	Gas products			Carbon balance (Carbon %)			
	CH ₄ (mmol) ^a	C ₂ H ₆ (mmol) ^a	H ₂ (mmol) ^a	Volatile liquids ^b	Non-volatile liquids ^c	Coke	Total
25	0	0	93.6	15.0	71.8	1.1	87.9
50	0	0	92.6	15.0	74.3	1.4	90.7
100	0.1	0	90.6	16.3	72.1	1.5	90.0
150	1.5	0.2	84.2	15.9	76.5	4.9	97.3

^a Calculated by multiplying the volume percentage of a specific gas by total moles of gas product assuming that all gases obey the ideal gas law.

^b Volatile liquids: distillates after rotary evaporation of liquid product at 55 °C and 2.47 psi (170 mbar) for 1 h.

^c Non-volatile liquids: distillation residue after rotor evaporation of liquid product at 55 °C and 2.47 psi (170 mbar) for 1 h.

pyrolytic lignin at 150 °C, from this the CH₄ and C₂H₆ are determined to be from ethanol. Lower CH₄ and C₂H₆ levels were produced with the pyrolytic lignin in ethanol than the pure ethanol probably because the pyrolytic lignin compounds can adsorb onto the Ru surface more strongly than the ethanol. In addition the pyrolytic lignin can form coke during the hydrogenation which can poison catalytic sites. Furthermore, after hydrogenation reactions 93-98% of the ethanol was recovered indicating the limited reactivity of ethanol.

Rotary evaporation was used to remove the solvent after reaction. As shown in Table 1, over 85% of the carbon from the pyrolytic lignin remained in the volatile or non-volatile liquid phases after hydrogenation for all the temperatures tested. The hydrogenation of pyrolytic lignin does not have a dramatic effect on the change of the product volatility. The coke yield slightly increased from 1.1 to 1.5% as the temperature increases from 25 to 100 °C. Furthermore, the coke yield increased to 4.9% as the temperature increases to 150 °C. As no coke formed during the reaction of the pure ethanol, ethanol was not the cause for coke formation. The non-volatile liquids of the hydrogenated pyrolytic lignin were analyzed by quantitative ¹³C NMR with the results shown in Figure 6. The percentages of carbonyl (including carboxyl), and aromatic carbons decrease by 31.9% and 11.9% respectively after hydrogenation at 25 °C demonstrating that hydrogenation begins at a low temperature. Increasing the reaction temperature to 50 °C, causes a 34.1% and 14.5% decrease from the feed in the carbonyl and aromatic carbons. More prominent decreases in carbonyl and aromatic carbons and increases in aliphatic C–O and C–C carbons are observed at the reaction temperatures of 100 °C and 150 °C. The percentage of aromatic carbon decreases from 65% in the pyrolytic lignin feed to 39% in the non-volatile liquids at 150 °C. The carbonyl and carboxyl group decrease from 6.5% to 2.0% and the percentage of aliphatic C–O and C–C bonds increase from 5.6% and 23.3% to 16.5% and 43.0% at the same reaction temperature. This indicates that unsaturated compounds are hydrogenated to saturated aliphatics.

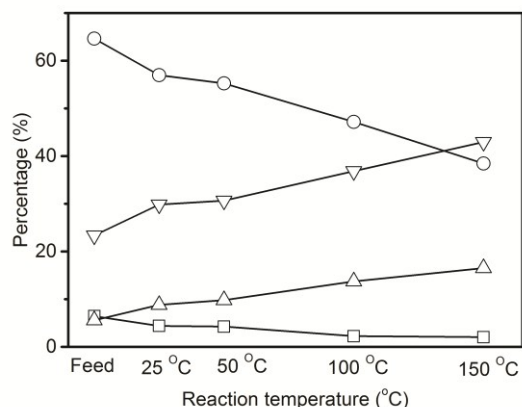


Figure 6. Quantitative ¹³C NMR results of non-volatile liquids from hydrogenation of pyrolytic lignin at various temperatures. Carbonyl and carboxyl region (□), aromatic region (○), aliphatic C–O region (Δ), and aliphatic C–C region (▽).

The quantitative ¹³C NMR spectra of the pyrolytic lignin feed and hydrogenated pyrolytic lignin at 150 °C was further analyzed to compare the carboxyl and other carbonyl functionality. In the quantitative ¹³C NMR spectra, 165-180 ppm corresponds to carboxyl group, while 180-215 ppm are attributed to other carbonyl groups.⁶² The peak area ratio of carboxyl groups to carbonyl groups change from 0.78:1 in pyrolytic lignin to 24.5:1 in hydrogenated pyrolytic lignin. This suggests that carbonyl groups are easier to hydrogenate than carboxyl functionalities. This is in agreement with literature results which shows that the rate of hydrogenation of carbonyl groups is about 80 times higher than the rate of hydrogenation of carboxyl groups with Ru catalysts.^{19,46,63}

The hydrogen balance for the run at 150 °C was calculated through NMR, pressure change, and GC gas product analyses. The hydrogen consumption was estimated to be 11.3 mmol by the change in pressure and gas composition. The stoichiometric hydrogen consumption calculated from the ¹³C NMR results and gas product analysis was calculated to be 9.3 mmol, within which 7.62 mmol was used to hydrogenate the non-volatile liquids. The overall hydrogen balance was 81.8%.

Though a pressure drop is observed after hydrogenation at 150 °C and cooling, the reactor pressure did not decrease with reaction time during the actual reaction (Supporting information Figure S2). This suggests that the catalytic reactions occurred at very short time periods and the coke poisoned the catalysts during the initial heating period.

Multistep hydrogenation of pyrolytic lignin

Hydrogenation of pyrolytic lignin was investigated using a multistep approach to understand the potential limitations of single-step hydrogenations. Table 2 highlights the carbon balances of the three step hydrogenation of pyrolytic lignin. In each of these experiments the product is separated from the spent catalyst and the hydrogenation reaction is repeated with fresh catalyst.

The amount of CH₄ and C₂H₆ produced increases with the number of hydrogenation steps. The carbon yield to coke is 1% after the second and the third step of the hydrogenation, which is nearly five times lower than after the first step. The carbon yield to volatile liquids increases from 15.9% in the first step to 26.7% in the third step, which implies that the pyrolytic lignin can undergo C–C bond hydrogenolysis to create more volatile compounds during this low temperature hydrogenation.

The quantitative ¹³C NMR results of the multistep hydrogenation are displayed in Figure 7. The percentages of carbonyl (including carboxyl), and aromatic carbons decrease and the percentages of aliphatic C–O and C–C moieties increase with additional hydrogenation steps. The percentage of carboxyl groups decrease from 1.9% after the first step hydrogenation to 1.6% after the second hydrogenation step and further decrease to 1.1% after the third hydrogenation. The S/G ratio increases from 1:2.4 to 1:1.8 after the second hydrogenation step. After the third hydrogenation step, almost no signals remained in the G or H regions, whereas signals in the S region were still present. Zhang et al.⁶⁴ carried out aqueous-

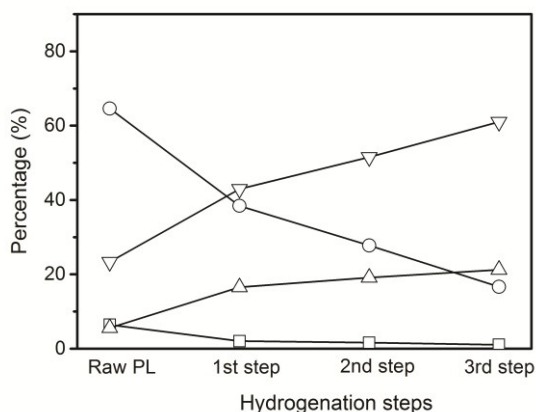


Figure 7. Quantitative ^{13}C NMR results of non-volatile liquids from multistep hydrogenation of pyrolytic lignin. Carbonyl and carboxyl region (□), aromatic region (○), aliphatic C–O region (Δ), aliphatic C–C region (▽)

phase hydrodeoxygenation of monomeric lignin model compounds including anisole, catechol, guaiacol and syringol over Ru/HZM-5 and observed the rate of hydrogenation of guaiacol was greater than that of syringol which is consistent with our results.

The ratio of C–O:C–C aliphatics is 0.24:1.00 in the pyrolytic lignin and changes to 0.38:1.00, 0.37:1.00, and 0.35:1.00 after the first, second, and third 150 °C hydrogenation respectively. The C–O:C–C aliphatic ratio increases with temperature from 0.24:1.00 in the feed

to 0.29:1.00, 0.32:1.00, 0.37:1.00, and 0.38:1.00 at 25, 50, 100, and 150 °C respectively.

The catalysts were recovered and the activity for hydrogenation of biphenyl was measured to compare the activity of the spent and fresh catalyst as shown in Table 3. The conversion of biphenyl was 69.3% over a fresh Ru/TiO₂ catalyst, whereas the conversion decreased to 7.4% over the Ru/TiO₂ after hydrogenation of pyrolytic lignin at 150 °C.

Furthermore, the selectivity to the fully hydrogenated product, bicyclohexyl, decreases over the recovered Ru/TiO₂. This result shows that Ru/TiO₂ deactivates after hydrogenation of pyrolytic lignin at 150 °C most likely due to coke forming on the catalyst surface. As the number of hydrogenation steps increases from 1 to 3, the conversion increases from 7.4% to 69.5%. This indicates that further hydrogenation steps decreases the coke formation. It also demonstrates that the remaining aromatics were harder to hydrogenate as the catalyst was still active towards biphenyl hydrogenation yet did not hydrogenate more of the aromatics

Hydrogenation of pyrolytic lignin fractions

The LMW and HMW fractions of the pyrolytic lignin were hydrogenated with Ru/TiO₂ at 150 °C as shown in Table 4 and Figure 8. Methane and ethane were produced in both experiments. According to the changes in pressure and gas composition, the hydrogen consumed during LMW fraction hydrogenation was 10.1 mmol, while that during HMW fraction hydrogenation was 6.4 mmol.

Table 2. Gas products and carbon balance of multistep hydrogenation of pyrolytic lignin (Reaction condition: 150 °C, 725 psig of initial H₂ pressure, 2.5 h reaction time, 10 g of pyrolytic lignin or hydrogenated pyrolytic lignin in ethanol (10 wt%), 1.50 g Ru/TiO₂).

Hydrogenation Step	Gas products				Carbon balance (Carbon %)		
	CH ₄ (mmol) ^a	C ₂ H ₆ (mmol) ^a	H ₂ (mmol) ^a	Volatile liquids ^b	Non-Volatile liquids ^c	Coke	Total
1 st hydrogenation	1.5	0.2	84.2	15.9	76.5	4.9	97.3
2 nd hydrogenation	4.0	0.3	85.1	21.1	72.6	1.0	94.7
3 rd hydrogenation	4.2	0.4	84.8	26.7	71.8	1.0	99.4

^a Calculated by multiplying the volume percentage of a specific gas by total moles of gaseous product assuming that all gases obey the ideal gas law.

^b Volatile liquids: distillates after rotor evaporation of liquid product at 55 °C and 170 mbar for 1 h.

^c Non-volatile liquids: distillation residue after rotor evaporation of liquid product at 55 °C and 170 mbar for 1 h.

Table 3. Hydrogenation of biphenyl with fresh and recovered catalyst (Reaction condition: 150 °C, 725 psig of initial H₂ pressure, 1 h reaction time, 10 g biphenyl in hexane (10 wt%), 80 mg of catalyst)

Catalyst	Conversion of Bip ^a (%)	Selectivity to Bic ^a (%)	Selectivity to Phc ^a (%)	Selectivity to unidentified (%)
Fresh Ru/TiO ₂	69.3	24.3	69.9	5.9
1 st Ru/TiO ₂ ^b	7.4	7.2	35.2	57.7
2 nd Ru/TiO ₂ ^c	25.7	17.6	68.6	13.8
3 rd Ru/TiO ₂ ^d	69.5	25.2	68.6	6.2

^a Bip: Biphenyl; Bic: Bicyclohexyl; Phc: Phenylcyclohexyl;

^b 1st Ru/TiO₂: recovered Ru/TiO₂ from the 1st hydrogenation step of pyrolytic lignin;

^c 2nd Ru/TiO₂: recovered Ru/TiO₂ from the 2nd hydrogenation step of pyrolytic lignin;

^d 3rd Ru/TiO₂: recovered Ru/TiO₂ from the 3rd hydrogenation step of pyrolytic lignin.

Table 4. Gas products and carbon balance of hydrogenation different fractions of pyrolytic lignin (Reaction condition: 150 °C of reaction temperature, 725 psig of initial H₂ pressure, 2.5 h reaction time, 10 g of pyrolytic lignin fractions (10 wt%), 1.50 g Ru/TiO₂).

Reaction feedstock	Gas products			Carbon balance (Carbon %)			
	CH ₄ (mmol) ^a	C ₂ H ₆ (mmol) ^a	H ₂ (mmol) ^a	Volatile liquids ^b	Non-volatile Liquids ^c	Coke	Total
LMW fraction ^d	0.5	0.05	85.4	N/A	87.4	3.9	91.3
HMW fraction ^e	0.6	0.04	89.0	25.4	63.5	7.7	96.6

^a Calculated by multiplying the volume percentage of a specific gas by total moles of gaseous product assuming that all gases obey the ideal gas law.

^b Volatile liquids: distillates from rotor evaporation of liquid product at 55 °C and 170 mbar for 1 h.

^c Non-volatile liquids: distillation residue from rotor evaporation of liquid product at 55 °C and 170 mbar for 1 h.

^d LMW fraction: low molecular weight fraction.

^e HMW fraction: high molecular weight fraction.

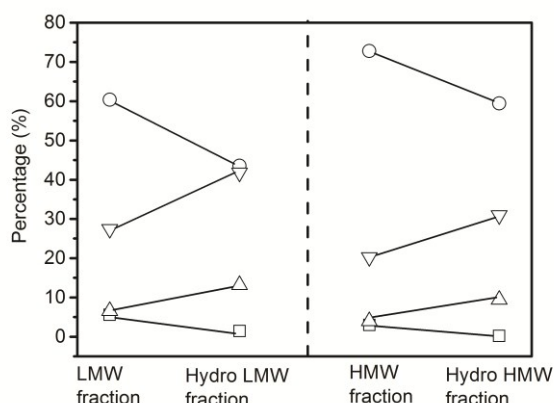


Figure 8. Quantitative ¹³C NMR results of non-volatile liquids from low molecular weight fraction (LMW fraction), high molecular weight fraction (HMW fraction), hydrogenated low molecular weight fraction (Hydro LMW fraction), and hydrogenated high molecular weight fraction (Hydro HMW fraction). Carbonyl and carboxyl bond (□), aromatic bond (○), aliphatic C–O bond (Δ), and aliphatic C–C bond (▽)

Hydrogenation of the LMW and HMW fractions did not change the distribution of volatile liquids and non-volatile liquids from the feedstock (Table S1). The coke yield from hydrogenation of the HMW fraction was 7.7%, which was nearly two times higher than the coke yield from the LMW fraction.

The quantitative ¹³C NMR results of the non-volatile liquids from the LMW fraction, the HMW fraction, and their respective hydrogenated products are shown in Figure 8. Compared with non-volatile liquids from HMW fraction, those from the LMW fraction contained more carbonyl, carboxyl, and aliphatic carbons but less aromatic carbons. After hydrogenation, the percentages of carbonyl, carboxyl, and aromatics decreased whereas the aliphatic carbons increased for the non-volatile liquids from both fractions. The percentage of aromatic carbons in the non-volatile liquids of LMW fraction decreased from 60.4% to 43.5% whereas in the non-volatile liquids of HMW fraction, decreased from 72.8% to 59.4%.

Pyrolytic lignin can be hydrogenated over a Ru/TiO₂ catalyst although catalyst deactivation due to coke formation is a major issue. The higher molecular weight compounds in pyrolytic lignin contribute more to the formation of coke than the lower molecular weight compounds. Along with the reduction in the formation of coke from further hydrogenation steps, this eludes to certain

molecules or functionalities in the molecules being responsible for, or more prone to, coke formation. To reduce the formation of coke a filtration or mild reaction may be necessary to remove or stabilize these compounds. Rover et al. demonstrated low pressure, low temperature hydrogenation over Pd/C to stabilize phenolic oligomers, a bio-oil fraction similar to pyrolytic lignin.²⁶ Another method to reduce coke formation during the hydrotreating would be to use a catalytic pyrolysis approach to produce the pyrolysis oil. Catalytic pyrolysis approaches may convert the most reactive part of the pyrolytic lignin thereby producing a pyrolysis oil that has a lower coke yield during hydrotreating than conventional pyrolysis oils produced with a non-catalytic approach.⁶⁵⁻⁷⁶

In this paper we start to understand some of the key classes of reactions that are occurring during hydrotreating of pyrolysis oils, but more advanced analytical approaches are needed to understand the complicated fundamental chemistry that is occurring during hydrogenation of pyrolytic lignin. These analytical approaches should be combined with theoretical and additional kinetic experiments to develop a molecular based model for hydrotreating of pyrolytic lignin. Free-radical reactions during the hydrotreating may be responsible for forming coke and, with this in mind, *in situ* electron paramagnetic resonance spectroscopy (EPR) could be an important technique to study the chemistry involved. More advanced mass spectrometric (MS) techniques capable of analyzing non-volatile substances could also be beneficial in understanding the chemistry of non-volatile pyrolytic lignin. Techniques such as Fourier transform ion cyclotron resonance mass spectrometry (FTICR-MS) and ion mobility mass spectrometry (IM-MS) are two MS techniques that allow for accurate detection of compounds without the need for volatilization that is required for other MS techniques.

Conclusions

Characterizations of pyrolytic lignin and hydrogenated pyrolytic lignin were performed utilizing 2D HSQC and quantitative ¹³C NMR analyses. The aromatic regions contained mainly guaiacyl and syringyl units, and low levels of *p*-hydroxyphenyl units whereas the aliphatic C–O region contained mainly methoxyl group peaks. β-aryl ether, phenylcoumaran, and resinol structures were not found in the pyrolytic lignin or products.

The hydrogenation of pyrolytic lignin over a Ru/TiO₂ catalyst converted a large amount of carboxyl/carbonyl and aromatic carbons into C–O and C–C aliphatic carbons. The G aromatics were easier to hydrogenate than the S aromatics. Hydrogenation was able to be carried out as low as 25 °C although coking still occurred at this temperature. Higher reaction temperatures increased both the degree of hydrogenation as well as formation of coke. Hydrogenation decreased the aromatic functionality 40.5% for a single-step and 74.2% for the three-step process. Hydrogenation of the HMW pyrolytic lignin fraction produced almost twice the coke yield as hydrogenation of the LMW pyrolytic lignin fraction. Understanding the cause of coke formation and developing techniques for mitigation of coke will be necessary for upgrading of pyrolytic lignin and pyrolysis oil as a whole.

Acknowledgements

The authors appreciate the financial support from China Scholarship Council. This work was also supported by the National Natural Science Foundation of China (51336008) and the Major State Basic Research Development Program of China (2013CB228100). JR and AA were funded by the DOE Great Lakes Bioenergy Research Center (DOE BER Office of Science DE-FC02-07ER64494). The authors would like to thank the Magnetic Resonance Facility in the Chemistry Department of the University of Wisconsin-Madison for use of the Bruker Advance III 500 gifted by Paul J. Bender.

References

- 1 A. V. Bridgwater, *Biomass and Bioenergy*, 2012, **38**, 68-94.
- 2 D. Meier, B. van de Beld, A. V. Bridgwater, D. C. Elliott, A. Oasmaa and F. Preto, *Renewable and Sustainable Energy Reviews*, 2013, **20**, 619-641.
- 3 C. Zhao and J. A. Lercher, *Angewandte Chemie International Edition*, 2012, **51**, 5935-5940.
- 4 M. Saidi, F. Samimi, D. Karimipourfard, T. Nimmanwudipong, B. C. Gates and M. R. Rahimpour, *Energy Environ. Sci.*, 2014, **7**, 103-129.
- 5 M. Ringer, V. Putsche and S. J., *Large-scale pyrolysis oil production: A technology assessment and economic analysis*, Report NREL/TP-510-37779, Midwest Research Institute, 2006.
- 6 M. M. Wright, D. E. Daugaard, J. A. Satrio and R. C. Brown, *Fuel*, 2010, **89**, S11-S19.
- 7 R. M. Swanson, A. Platon, J. A. Satrio and R. C. Brown, *Fuel*, 2010, **89**, S2-S10.
- 8 R. P. Anex, A. Aden, F. K. Kazi, J. Fortman, R. M. Swanson, M. M. Wright, J. A. Satrio, R. C. Brown, D. E. Daugaard, A. Platon, G. Kothandaraman, D. D. Hsu and A. Dutta, *Fuel*, 2010, **89**, S29-S35.
- 9 E. Furimsky, *Appl Catal a-Gen*, 2000, **199**, 147-190.
- 10 D. C. Elliott, *Energy Fuel*, 2007, **21**, 1792-1815.
- 11 J. Wildschut, F. H. Mahfud, R. H. Venderbosch and H. J. Heeres, *Ind Eng Chem Res*, 2009, **48**, 10324-10334.
- 12 J. Wildschut, I. Melian-Cabrera and H. J. Heeres, *Appl Catal B-Environ*, 2010, **99**, 298-306.
- 13 E. Butler, G. Devlin, D. Meier and K. McDonnell, *Renew Sust Energy Rev*, 2011, **15**, 4171-4186.
- 14 P. M. Mortensen, J. D. Grunwaldt, P. A. Jensen, K. G. Knudsen and A. D. Jensen, *Appl Catal a-Gen*, 2011, **407**, 1-19.
- 15 D. Mohan, C. U. Pittman and P. H. Steele, *Energy Fuel*, 2006, **20**, 848-889.
- 16 C. R. Vitasari, G. W. Meindersma and A. B. de Haan, *Bioresource Technol*, 2011, **102**, 7204-7210.
- 17 T. P. Vispute and G. W. Huber, *Green Chem*, 2009, **11**, 1433-1445.
- 18 T. P. Vispute, H. Y. Zhang, A. Sanna, R. Xiao and G. W. Huber, *Science*, 2010, **330**, 1222-1227.
- 19 J. C. Lee, Y. Xu and G. W. Huber, *Appl Catal B-Environ*, 2013, **140**, 98-107.
- 20 J. Lee, Y. T. Kim and G. W. Huber, *Green Chem*, 2014, **16**, 708-718.
- 21 C. A. Mullen and A. A. Boateng, *Journal of Analytical and Applied Pyrolysis*, 2011, **90**, 197-203.
- 22 H. X. Ben, W. Mu, Y. L. Deng and A. J. Ragauskas, *Fuel*, 2013, **103**, 1148-1153.
- 23 M. Garcia-Perez, A. Chaala, H. Pakdel, D. Kretschmer and C. Roy, *Biomass Bioenergy*, 2007, **31**, 222-242.
- 24 N. Ozbay, A. E. Putun and E. Putun, *Int J Energy Res*, 2006, **30**, 501-510.
- 25 A. E. Putun, B. B. Uzun, E. Apaydin and E. Putun, *Fuel Process Technol*, 2005, **87**, 25-32.
- 26 M. R. Rover, P. H. Hall, P. A. Johnston, R. G. Smith and R. C. Brown, *Fuel*, 2015, **153**, 224-230.
- 27 B. Scholze, C. Hanser and D. Meier, *Journal of Analytical and Applied Pyrolysis*, 2001, **58-59**, 387-400.
- 28 A. Oasmaa, E. Kuoppala, S. Gust and Y. Solantausta, *Energy Fuel*, 2003, **17**, 1-12.
- 29 A. Oasmaa, E. Kuoppala and Y. Solantausta, *Energy Fuel*, 2003, **17**, 433-443.
- 30 L. Ingram, D. Mohan, M. Bricka, P. Steele, D. Strobel, D. Crocker, B. Mitchell, J. Mohammad, K. Cantrell and C. U. Pittman, *Energy Fuel*, 2008, **22**, 614-625.
- 31 H. Ben and A. J. Ragauskas, *Energy Fuel*, 2011, **25**, 2322-2332.
- 32 S. D. Mansfield, H. Kim, F. Lu and J. Ralph, *Nature protocols*, 2012, **7**, 1579-1589.
- 33 T. Q. Yuan, S. N. Sun, F. Xu and R. C. Sun, *Journal of agricultural and food chemistry*, 2011, **59**, 10604-10614.
- 34 H. Kim and J. Ralph, *Organic & biomolecular chemistry*, 2010, **8**, 576-591.
- 35 B. Scholze and D. Meier, *Journal of Analytical and Applied Pyrolysis*, 2001, **60**, 41-54.
- 36 R. Bayerbach, V. D. Nguyen, U. Schurr and D. Meier, *Journal of Analytical and Applied Pyrolysis*, 2006, **77**, 95-101.
- 37 R. Bayerbach and D. Meier, *Journal of Analytical and Applied Pyrolysis*, 2009, **85**, 98-107.
- 38 *US Pat.*, 7578927, 2009.
- 39 T. Zhe, Z. Ying and G. Qingxiang, *Ind Eng Chem Res*, 2010, **49**, 2040-2046.
- 40 T. Prasomsri, M. Shetty, K. Murugappan and Y. Román Leshkov, *Energy & Environmental Science*, 2014, **7**, 2660.

- 41 J. Zakzeski, P. C. A. Bruijninx, A. L. Jongerius and B. M. Weckhuysen, *Chem Rev*, 2010, **110**, 3552-3599.
- 42 D. C. Elliott, H. Wang, M. Rover, L. Whitmer, R. Smith and R. Brown, *ACS Sustainable Chemistry & Engineering*, 2015, **3**, 892-902.
- 43 *US Pat.*, 20080006519, 2008.
- 44 *US Pat.*, 20080006520, 2008.
- 45 J. Wildschut, M. Iqbal, F. H. Mahfud, I. M. Cabrera, R. H. Venderbosch and H. J. Heeres, *Energy & Environmental Science*, 2010, **3**, 962.
- 46 H. Olcay, L. J. Xu, Y. Xu and G. W. Huber, *Chemcatchem*, 2010, **2**, 1420-1424.
- 47 J. Duan, Y. T. Kim, H. Lou and G. W. Huber, *Catalysis Today*, 2014, **234**, 66-74.
- 48 J. C. del Rio, J. Rencoret, G. Marques, A. Gutierrez, D. Ibarra, J. I. Santos, J. Jimenez-Barbero, L. M. Zhang and A. T. Martinez, *Journal of agricultural and food chemistry*, 2008, **56**, 9525-9534.
- 49 J. C. del Rio, J. Rencoret, G. Marques, J. B. Li, G. Gellerstedt, J. Jimenez-Barbero, A. T. Martinez and A. Gutierrez, *Journal of agricultural and food chemistry*, 2009, **57**, 10271-10281.
- 50 J. J. Villaverde, J. B. Li, M. Ek, P. Ligerio and A. de Vega, *Journal of agricultural and food chemistry*, 2009, **57**, 6262-6270.
- 51 F. C. Lu and J. Ralph, *Plant J*, 2003, **35**, 535-544.
- 52 F. C. Lu, J. Ralph, K. Morreel, E. Messens and W. Boerjan, *Organic & biomolecular chemistry*, 2004, **2**, 2888-2890.
- 53 J. Rencoret, G. Marques, A. Gutierrez, L. Nieto, J. Jimenez-Barbero, A. T. Martinez and J. C. del Rio, *Ind Crop Prod*, 2009, **30**, 137-143.
- 54 T. Q. Yuan, S. N. Sun, F. Xu and R. C. Sun, *Journal of agricultural and food chemistry*, 2011, **59**, 6605-6615.
- 55 J. C. del Rio, J. Rencoret, P. Prinsen, A. T. Martinez, J. Ralph and A. Gutierrez, *Journal of agricultural and food chemistry*, 2012, **60**, 5922-5935.
- 56 P. Pandey M and S. Kim C, *Chemical Engineering & Technology*, 2011, **34**, 29-41.
- 57 S. Chu, A. V. Subrahmanyam and G. W. Huber, *Green Chem*, 2013, **15**, 125-136.
- 58 P. R. Patwardhan, R. C. Brown and B. H. Shanks, *Chemsuschem*, 2011, **4**, 1629-1636.
- 59 P. Karhunen, P. Rummakko, J. Sipilä, G. Brunow and I. Kilpeläinen, *Tetrahedron Lett.*, 1995, **36**, 169-170.
- 60 J. Ralph and L. L. Landucci, in *Lignin and Lignans; Advances in Chemistry*, eds. C. Heitner, D. R. Dimmel and J. A. Schmidt, CRC Press (Taylor & Francis Group), Boca Raton, FL, 2010, ch. 5, pp. 137-234.
- 61 A. R. Teixeira, K. G. Mooney, J. S. Kruger, C. L. Williams, W. J. Suszynski, L. D. Schmidt, D. P. Schmidt and P. J. Dauenhauer, *Energy & Environmental Science*, 2011, **4**, 4306.
- 62 C. A. Mullen, G. D. Strahan and A. A. Boateng, *Energ Fuel*, 2009, **23**, 2707-2718.
- 63 H. Olcay, Y. Xu and G. W. Huber, *Green Chem*, 2014, **16**, 911-924.
- 64 W. Zhang, J. Chen, R. Liu, S. Wang, L. Chen and K. Li, *ACS Sustainable Chemistry & Engineering*, 2014, 140107152122009.
- 65 V. Paasikallio, C. Lindfors, E. Kuoppala, Y. Solantausta, A. Oasmaa, J. Lehto and J. Lehtonen, *Green Chem*, 2014, **16**, 3549.
- 66 E. F. Iliopoulou, S. Stefanidis, K. Kalogiannis, A. C. Psarras, A. Delimitis, K. S. Triantafyllidis and A. A. Lappas, *Green Chem.*, 2014, **16**, 662-674.
- 67 E. F. Iliopoulou, E. V. Antonakou, S. A. Karakoulia, I. A. Vasalos, A. A. Lappas and K. S. Triantafyllidis, *Chem Eng J*, 2007, **134**, 51-57.
- 68 F. A. Agblevor, S. Beis, O. Mante and N. Abdoulmoumine, *Ind Eng Chem Res*, 2010, **49**, 3533-3538.
- 69 F. A. Agblevor, O. Mante, N. Abdoulmoumine and R. McClung, *Energ Fuel*, 2010, **24**, 4087-4089.
- 70 *US Pat.*, 8,669,405, 2014.
- 71 *US Pat.*, 8,377,152, 2013.
- 72 *US Pat.*, 8,927,793, 2015.
- 73 *US Pat.*, 8,519,203, 2013.
- 74 M. Biddy, A. Dutta, S. Jones and A. Meyer, *Ex-Situ catalytic fast pyrolysis technology pathway*, Report PNNL-22317, National Renewable Energy Laboratory and Pacific Northwest National Laboratory, 2013.
- 75 M. Biddy, A. Dutta, S. Jones and A. Meyer, *In-Situ catalytic fast pyrolysis technology pathway*, Report PNNL-22320, National Renewable Energy Laboratory and Pacific Northwest National Laboratory, 2013.
- 76 A. Dutta, A. Sahir, E. Tan, D. Humbird, L. J. Snowden-Swan, P. Meyer, J. Ross, D. Sexton, R. Yap and J. Lukas, *Process design and economics for the conversion of lignocellulosic biomass to hydrocarbon fuels: Thermochemical research pathways with In Situ and Ex Situ upgrading of fast pyrolysis vapors*, Report PNNL-23823, National Renewable Energy Laboratory and Pacific Northwest National Laboratory, 2015.

Graphical Abstract

The low temperature hydrogenation of pyrolytic lignin over Ru/TiO₂ was studied and characterized with quantitative ¹³C and 2D ¹H-¹³C HSQC NMR to determine the changes in carbon functionality.

